Proceedings of the
International Conference on Mechanical Engineering 2009
(ICME2009) 26- 28 December 2009, Dhaka, Bangladesh

ICME09-FM-11

NUMERICAL SIMULATION OF A CONFINED LAMINAR DIFFUSION FLAME WITH VARIABLE PROPERTY FORMULATION

B. K. MANDAL [1], **A.K. CHOWDHURI** [1] **and A. J. BHOWAL** [2]

[1]Bengal Engineering and Science University, Howrah, India
[2]Heritage Institute of Technology, Kolkata, India

ABSTRACT

A numerical model is used for simulation of a confined axisymmetric laminar jet diffusion flame under normal gravity and pressure conditions to predict the velocity, temperature and species distributions. An explicit finite difference technique has been adopted for the numerical simulation of reacting flow with finite rate chemistry and variable thermodynamic and transport properties. The predictions match well with the experimental results available in the literature. A recirculation of ambient air is observed to extend from the exit plane into the domain adjacent to the wall. Radial velocity is never positive (away from the axis) in the solution domain. High temperature and high CO_2 concentration zone are confined to a small radial distance.

Keywords: Diffusion flame, Recirculation, Temperature distribution.

1. INTRODUCTION

The numerical simulation is a useful tool because it can easily employ various conditions by simply changing the parameters. Confined diffusion flames are commonly found in practical combustion systems, such as the power-plant combustor, gas turbine combustor, and jet engine afterburner. In these systems, fuel is injected into a duct with a co-flowing or cross-flowing air stream. The diffusion flame is found at the surface where the fuel jet and oxygen meet, react, and consume each other. The overall combustion in such situations is governed by a complex interaction of chemical reactions, transport and gas dynamic processes that are strongly dependent on physical boundary conditions and the type of the chemical system. The ability to predict the coupled effects of various complex transport processes and chemical kinetics in these systems is critical in obtaining velocity, temperature and different species concentration distributions. Computer simulation of the combustion process enables the prediction of optimal operating conditions for achieving high combustion efficiency and low emissions in the exhaust, and aids in the development of optimal burner designs.

Experimental and numerical investigations of steady confined laminar diffusion flame were carried out by Mitchell *et al.* [1] to study the temperature, velocity and concentration profiles of stable species. Smooke *et al.* [2] obtained the numerical solution of the two-dimensional axi-symmetric laminar co-flowing jet diffusion flame of methane and air both in the confined and the unconfined environment. A numerical simulation of an axi-symmetric confined diffusion flame formed between a H_2-N_2 jet and co-flowing air, each at a velocity of 30 cm/s, were presented by Ellzey *et al*. [3]. Li *et al.* [4] investigated a highly over-ventilated laminar co-flow diffusion flame in axi-symmetric geometry considering unity Lewis number and the effects of buoyancy. Katta *et al.* [5] developed a time dependent, axi-symmetric H_2-air diffusion flame model to study the effects of Lewis number and finite rate chemistry on the steady state and dynamic flame structures.

The simulation described here is pertinent to laboratory scale studies of diffusion flames in burners commonly referred to as Wolkard bumers, A numerical model was constructed for the purpose of understanding the interplay of diffusion, convection and chemical kinematics. In the present formulation, finite rate chemistry as well as the non-unity Lewis number and property variation have been considered.

The combustion system considered is the laminar diffusion flame in a confined physical environment with co-flowing fuel and air (oxidizer) streams. Two concentric vertical tubes comprise the burner. The fuel is admitted as a central jet through the inner tube and air as a co-flowing annular jet through the outer tube. The inner fuel tube diameter is 12.7 mm and the outer tube diameter is 50.4 mm. The thickness of the inner tube wall is neglected here. The dimensions are in conformity with the earlier experimental work of Mitchell *et al.* [1] and the numerical work of Smooke *et al.* [2]. The two

streams diffuse into each other at the outlet of the inner tube in order to produce a flammable mixture of fuel and air. A cylindrical shield of diameter 50.4 mm defines an impervious outer boundary (wall) of the axisymmetric system. The length of the computational domain in the axial direction is taken to be 30 cm.

2. NUMERICAL MODEL

The combustion process is simulated with a detailed numerical model, solving the governing equations for reacting flow with appropriate boundary conditions. The flow is assumed to be laminar and axi-symmetric produced by a jet of fuel emerging from a circular nozzle, which burns in a co-flowing stream of air in a confined environment. The reaction between the fuel and oxidizer proceeds through two-step irreversible chemical reactions. The flow is vertical through the reaction space and the gravity effect is included in the momentum equation. A variable property formulation has been made for the transport and thermodynamic properties. The radiation heat exchange within the gas phase is neglected because the soot loading with methane fuel is low. The Soret effect due to thermal diffusion is also neglected. Considering the axi-symmetric geometry, the numerical simulations have been performed on one side of the axis.

2.1 Governing Equations

The description of a problem in combustion can be given by the conservation equations of mass, momentum, species concentrations and energy. The gas phase conservation equations in cylindrical co-ordinate system have been used to model the reacting flow. The conservation equations with transient terms for mass, radial momentum, axial momentum, species concentrations and energy are presented in Eq.(1) to Eq.(5) respectively.

$$\frac{\partial \rho}{\partial t} + \frac{1}{r}\frac{\partial}{\partial r}(r \rho v_r) + \frac{\partial}{\partial z}(\rho v_z) = 0 \qquad (1)$$

$$\frac{\partial}{\partial t}(\rho v_r) + \frac{1}{r}\frac{\partial}{\partial r}\left(r \rho v_r^2\right) + \frac{\partial}{\partial z}(\rho v_r v_z) = -\frac{\partial p}{\partial r} + \frac{2}{r}\frac{\partial}{\partial r}\left(r \mu \frac{\partial v_r}{\partial r}\right) - \frac{2}{r}\mu\frac{v_r}{r^2} + \frac{\partial}{\partial z}\left\{\mu\left(\frac{\partial v_z}{\partial r} + \frac{\partial v_r}{\partial z}\right)\right\} - \frac{2}{3}\frac{\partial}{\partial r}\left(\mu\left(\frac{\partial v_r}{\partial r} + \frac{v_r}{r} + \frac{\partial v_z}{\partial z}\right)\right) \qquad (2)$$

$$\frac{\partial}{\partial t}(\rho v_z) + \frac{1}{r}\frac{\partial}{\partial r}(r \rho v_r v_z) + \frac{\partial}{\partial z}\left(\rho v_z^2\right) = -\frac{\partial p}{\partial z} + \frac{1}{r}\frac{\partial}{\partial r}\left\{r \mu\left(\frac{\partial v_z}{\partial r} + \frac{\partial v_r}{\partial z}\right)\right\} + 2\frac{\partial}{\partial z}\left(\mu\frac{\partial v_z}{\partial z}\right) - \frac{2}{3}\frac{\partial}{\partial z}\left\{\mu\left(\frac{\partial v_r}{\partial r} + \frac{v_r}{r} + \frac{\partial v_z}{\partial z}\right)\right\} + \rho g \qquad (3)$$

$$\frac{\partial}{\partial t}(\rho C_j) + \frac{1}{r}\frac{\partial}{\partial r}(r \rho v_r C_j) + \frac{\partial}{\partial z}(\rho v_z C_j) = \frac{1}{r}\frac{\partial}{\partial r}\left(r \rho D_{jm}\frac{\partial C_j}{\partial r}\right) + \frac{\partial}{\partial z}\left(\rho D_{jm}\frac{\partial C_j}{\partial z}\right) + \dot{S}_{cj} \qquad (4)$$

$$\frac{\partial}{\partial t}(\rho h) + \frac{1}{r}\frac{\partial}{\partial r}(r \rho v_r h) + \frac{\partial}{\partial z}(\rho v_z h) = \frac{1}{r}\frac{\partial}{\partial r}\left(r\frac{\lambda}{c_p}\frac{\partial h}{\partial r}\right) + \frac{\partial}{\partial z}\left(\frac{\lambda}{c_p}\frac{\partial h}{\partial z}\right) + \frac{1}{r}\frac{\partial}{\partial r}\left[r\frac{\lambda}{c_p}\sum_{j=1}^{n} h_j\left(Le_j^{-1} - 1\right)\frac{\partial C_j}{\partial r}\right] + \frac{\partial}{\partial z}\left[\frac{\lambda}{c_p}\sum_{j=1}^{n} h_j\left(Le_j^{-1} - 1\right)\frac{\partial C_j}{\partial z}\right] \qquad (5)$$

where, C_j is the mass fraction of the respective species and D_{jm} is the diffusion coefficient of the species in a binary mixture of that species and nitrogen and Le_j is the local Lewis number defined as

$$Le_j = \frac{\lambda}{c_p}\frac{1}{\rho D_{jm}} \qquad (6)$$

The source term, $\dot{S}_{cj}$ appearing in Eq.(4) is the rate of production or destruction of the species j per unit volume due to chemical reaction. The temperature dependence of viscosity (μ), thermal conductivity (λ), mass diffusivity (D_{jm}) and specific heat (c_p) has been taken into account using suitable correlations available in the literature. The axial and radial directions are denoted by z and r respectively. The conservation equation for chemical species is solved for five gaseous species, viz. CH_4, O_2, CO_2, CO and H_2O. The concentration for N_2 is obtained by difference.

2.2 Boundary Conditions

Boundary conditions at the inlet are given separately for the fuel stream at the central jet and the air stream at the annular co-flow. The streams are considered to enter the computational domain as plug flow, with velocities calculated from their respective mass flow rates. The temperatures of fuel and air are specified. In conformation with the conditions used by Mitchell *et al.* [1] and Smooke *et al.* [2], the fuel flow rate is taken as 3.71×10^{-6} kg/s and the air flow rate is taken as 2.214×10^{-4} kg/s. Considering the length of the computational domain to be 0.3 m, the fully developed boundary conditions for the variables are considered at the outlet. In case of reverse flow at the outlet plane, which occurs in the case of buoyant flame, the stream coming in from the outside is considered to be ambient air. Axi-symmetric condition is considered at the central axis, while at the wall a no-slip, adiabatic and impermeable boundary condition is adopted.

2.3 Solution Methodology

The conservation equations of mass, momentum, energy and species concentrations are solved simultaneously, with their appropriate boundary conditions, by an explicit finite difference computing technique. The solution yields velocity, temperature, and

species concentration. The numerical scheme adopted for solving the reacting flow problem is based on a straight-forward, yet powerful algorithm called SOLA (Solution Algorithm) developed by Hirt and Cook [6]. The algorithm is based on primitive variables and the variables are defined following a staggered grid arrangement. The solution is explicitly advanced in time till a steady state convergence is achieved. A variable size adaptive grid system is considered using hyperbolic distribution to capture the sharp gradients of the field variables. After extensive grid independence test, an optimal numerical mesh with 85×41 grid nodes is finally adopted. The diffusion terms are discretized by a central differencing scheme, whereas the advection terms are discretized by a hybrid differencing schemes as described by Patankar [7]. The fluid properties like density, specific heat and viscosity are calculated at the cell faces by linear interpolation between the corresponding property values at the adjacent cell centres. The source terms are considered to be constant throughout the volume of each cell. The ignition of the fuel-air mixture in the combustion chamber is simulated by raising the temperature of the mixture within a few cells, to 1000 K, near the fuel-air interface (slightly above the burner tip) and maintaining till the local temperature of the mixture is raised beyond the ignition temperature due to reaction.

3. RESULTS AND DISCUSSION

The predictions from the present simulation are compared with the experimental results of Mitchell *et al.* [1] for the same operating conditions. Radial distributions of temperature and major product species (CO_2 and H_2O) concentrations at a height of 12 mm above the burner rim are shown in Fig. 1(a) and Fig. 1(b) respectively. Clearly the figures show a good agreement between the predicted values and experimental values of Mitchell *et al.* [1].

Combustion in diffusion mode is simulated with air of inlet temperature 300 K and also methane (fuel) of inlet temperature 300 K. The shape and size of the steady state flame in the computational zone is shown in Fig. 2 with the help of flame front. The investigation shows that the steady state flame has an over-ventilated shape.

3.1 Velocity Distributions

The velocity field has been described by showing the axial velocity and radial velocity distributions at six different axial heights, z, above the burner. The axial heights, considered here are 2 cm, 6 cm, 10 cm, 15 cm, 20 cm and 30 cm. Figures 3 and 4 show variations of axial velocity and radial velocity with radial distance from the centreline at the above mentioned axial heights. Figure 3 clearly depicts that the axial velocity around the central region is high and also increases with height. The maximum centreline axial velocity at the exit plane is as high as 4.0 m/s. The axial velocity away from the centreline decreases at all heights and becomes very low beyond a radial distance of 0.015 m. It is also interesting to note that the axial velocity becomes negative above an axial position of 10 cm upto the exit plane (30 cm). This indicates that ambient air from the exit plane is entering into the computational domain near the pheriphery. This penetrates upto a depth of 20 cm from the exit plane and a large recirculation from outside is noted.

Figure 4 shows that the radial velocity is always negative (i.e. towards the centre) except at the exit plane. This also confirms the presence of the recirculation from the exit plane near wall. There is also entrainment of air from the air side to the reaction zone. The maximum negative value of radial velocity at a radial position of around 0.0065 m indicates that the entrainment is more near the fuel-air interface. It is also clear that the entrainment is maximum at a lower axial position of 2 cm. The recirculation zone acts a barrier for the upward motion of the gas mixture towards the exit plane. Also the high temperatures in the reaction zone within the flame sets strong buoyant force near the axis. All these facts together explain the presence of high axial velocity near the axis. Also as the air is entering from the exit plane near the wall, the velocity in the central zone has to be high to satisfy the continuity equation.

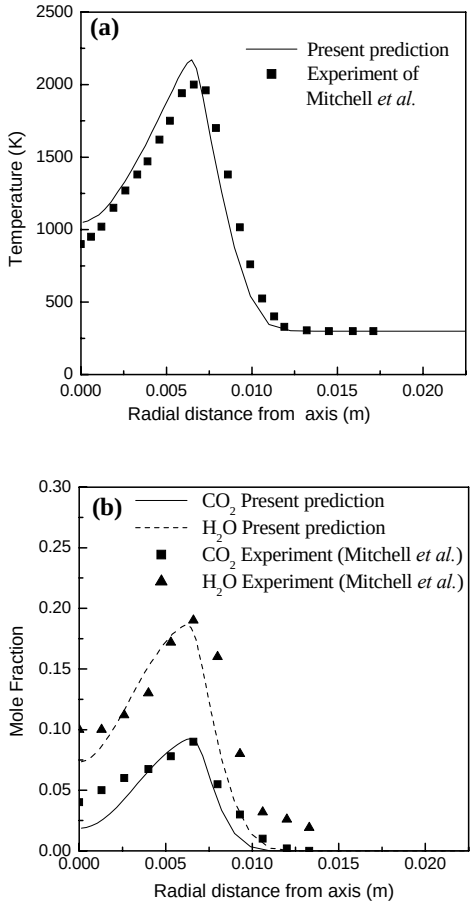

Fig 1. Comparison of the radial (a) temperature (b) species (CO_2 and H_2O) distributions at 12 mm axial height above the burner

3.2 Temperature Distributions

The temperature distributions for the diffusion flame have been described in Fig. 5 by plotting temperature as a function of radial distance from the centreline for different axial positions mentioned earlier. The temperature distributions as shown in figure 5 indicate that high temperature zone is limited only upto a certain

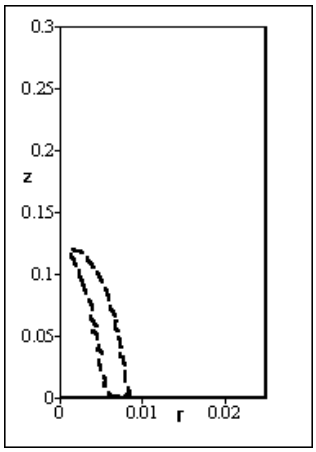

Fig.2. Shape and size of the flame

radial position (approx. 0.007 m) for all axial positions. Beyond that the temperature remains very low (almost 300 K). This is due to the recirculation of ambient air from the exit plane. The maximum temperature observed in this case is about 2250 K at an axial position of 10 cm. Above this the temperature becomes lower. This indicates that the flame height is in between 10 cm and 15 cm. Also , from z = 2 to 10 cm, the radial position of the maximum temperature shifts towards the axis confirming the overventilated flame shape under the present operating condition. The temperature values in the high temperature regions are overpredicted by 50-100 K. This may be attributed to the fact that the present model has not considered the radiative exchange.

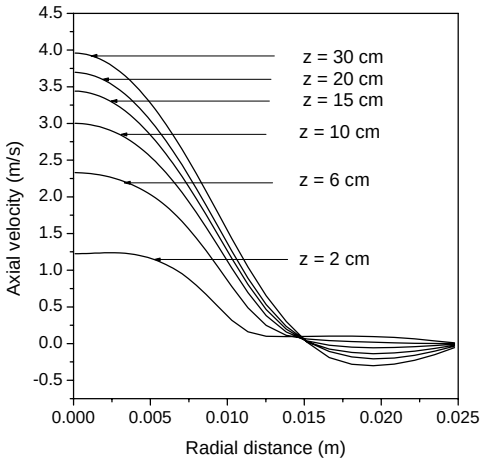

Fig. 3. Radial distributions of axial velocity at different axial heights, z.

3.3 Species Concentrations

The radial distributions of CO_2 (one of the major product species) have been shown for different axial positions in Fig. 4. The peak values of CO_2 concentration decrease after an axial position of 10 cm indicating the reaction zone to be limited to around 10 cm in the axial direction. The trend of CO_2 distributions has a similarity with the temperature distributions. CO_2 is present only in the high temperature zone, i.e., within the flame and above the flame. The concentration decreases above the flame due to the entrainment of ambient air entering through the exit plane near the wall.

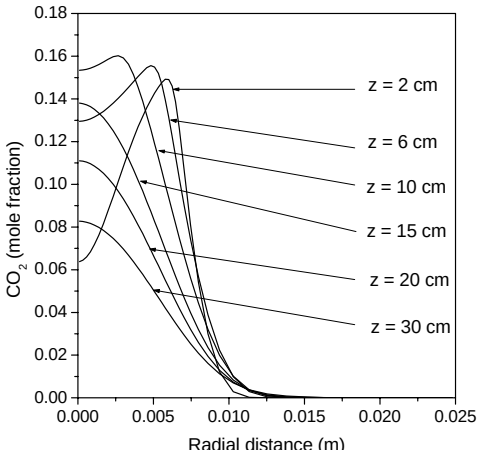

Fig 4. Radial distributions of CO_2 concentrations at different axial heights, z.

4. CONCLUSION

Numerical computations of axisymmetric laminar diffusion flame for methane in air have been carried out to examine the nature of flame shape, distributions of velocity, temperature, and different species concentrations in a confined geometry. Initial conditions for diffusion flame for methane and air correspond to 300 K and 0.1 MPa. Different conservation equations for mass, momentum, energy and species concentration for reacting flows are solved in an axisymmetric cylindrical co-ordinate system. A two-steps chemical reaction of methane and air (oxidizer) has been considered to capture some of the features of chemical reaction mechanisms. The CFD model based on SOLA algorithm predicts velocity, temperature and species distributions throughout the computational zone of the cylindrical burner having the dimensions of 30 cm (axial length), 12.7 mm (inner diameter) and 50.4 mm (outer diameter). The predictions from the model match well with the experimental results available in the literature. The research results show that the highest calculated value of temperature near the flame tip is of the order of 2250 K, which is slightly overpredicted. The velocity distributions show that the fluid elements near the axis have been accelerated due to strong buoyant force. There is a recirculation of atmospheric air from the exit plane near the wall. As a result, the temperature near the wall is almost atmospheric temperature of 300 K. The higher temperature zone is confined only around the axis only.

The CO_2 concentration distribution characteristics are almost same as that of temperature distributions. It can be concluded that the present model of two-steps reaction mechanism is fairly useful for determining the combustion characteristics of laminar diffusion flame.

5. REFERENCES

1. Mitchell, R. E., Sarofim, A. F. and Clomburg, L. A., 1980, "Experimental and Numerical Investigation of Confined Laminar Diffusion Flames", Combustion and Flame, 37: 227 -244.
2. Smooke, M. D., Mitchell, R. E. and Keys, D. E., 1989, "Numerical Solution of Two-Dimensional Axisymmetric Laminar Diffusion Flames", Combustion Science and Technology, 67: 85 - 122.
3. Ellzey, J. L., Laskey, K. J. and Oran, E. S., 1991, "A Study of Confined Diffusion Flames", Combustion and Flame, 84**:** 249-264.
4. Li, S. C., Gordon, A. S. and Williams, F. A., 1995, "A Simplified Method for the Computation of Burke-Schumann Flames in Infinite Atmospheres", Combustion Science and Technology, 104: 75 – 91.
5. Katta, V. R., Goss, L. P. and Roquemore, W.M., 1994, "Effect of Nonunity Lewis Number and Finite Rate Chemistry on the Dynamics of Hydrogen- Air Jet Diffusion Flame", Combustion and Flame, 96: 60 - 74.
6. Hirt, C. W. and Cook, J. L. 1972, "Calculating Three-Dimensional Flows Around Structures and over Rough Terrain", Journal of Computational Physics, 10 : 324 – 338.
7. Patankar, S. V., 1980, " Convection and Diffusion", *Numerical Heat Transfer and Fluid Flow*. Hemispherical Publishing Corporation.

6. NOMENCLATURE

Symbol	Meaning	Unit
C_i	Concentration of jth species	--
c_p	Specific heat	J/kgK
D	Mass diffusivity	m^2/s
g	Acceleration due to gravity	m/s^2
h	Enthalpy	J/kg
Le	Lewis number	--
p	Pressure	Pa
r	Radial distance	m
T	Temperature	K
t	Time	s
v	Velocity	m/s
z	Axial distance	m
μ	Viscosity	kg/ms
ρ	Density	kg/m^3
λ	Thermal conductivity	W/mK

7. MAILING ADDRESS

Prof. Bijan Kumar Mandal
Department of Mechanical Engineering
Bengal Engineering and Science University, Shibpur
Howrah-711103, INDIA.
Phone : 91-033-26887619
91-033- 26684562-64 (Extn. 279)
FAX : 91-033-26684561
E-mail : bijan@mech.becs.ac.in
bkm375@yahoo.co.in